

Hot Pixel Generation in Active Pixel Sensors: Dosimetric and Microdosimetric response

ABSTRACT--The dosimetric and microdosimetric response of an active pixel sensor is analyzed. The shift in dark current before and after irradiation is the metric under study. Heavy ions are seen to damage the pixel in much the same way as proton radiation, i.e., displacement damage is the dominant mechanism. A rate of singularly highly dosed cells, i.e. hot pixels, is calculated from the distribution of dosed cells. The probability of a hot pixel is seen to exhibit behavior that is not typical of other microdose effects. The cross section of hot pixels is seen to increase with increasing NIEL.

I. INTRODUCTION

CMOS active pixel sensors are being employed more often in space imaging application due to moderate noise performance and ease of use. Mission profiles are also becoming more complex. An APS device may endure radiation from electrons, protons, neutrons, and heavy ions over several different missions or a single mission. This diversity of environments makes the designing around the radiation effects somewhat challenging. Since star scanning missions, which employ on the APS, rely on the integrity of each cell of the device, the effects on a single imaging cell must likewise be studied [1]-[2].

APS cells can be accessed directly, so charge transfer efficiency degradation issues experienced from radiation damage can be avoided. Readout circuitry in APS devices has become more complex to increase ability on chip and this has introduced new radiation effects. Part of the light collection circuit in an APS is either a photodiode or a photogate, but in either case the light collection is a lightly doped reversed biased junction. APS devices have transistors that function as access or reset switches or current gates. The dark current will increase with radiation dose in the light collection area and the support transistors [1]-[5].

Since the increase in dark current due to radiation damage is equivalent to a false signal, missions often incorporate mitigation strategies to reduce false images from dark current increase. For TID and DD offset, the strategy is predicting and increasing integration time. An increase in the false signal of an individual bit requires a more challenging solution, however. A re-measurement of the background is commonly employed, but the rate is unknown for various environments since the response of APS cells to heavy ions is not well known. This study investigates the individual response of APS cells to heavy radiation and determines the equivalent amount of displacement damage that a heavy ion strike induces.

II. THEORY

¹ Manuscript received September 12, 2003. The research in this paper was carried out by the Jet Propulsion Laboratory, California Institute of Technology under contract with the National Aeronautics and Space Administration (NASA) Code AE, under the Electronic Parts and Packaging Program (NEPP).

L. Sscheck and L. Edmonds are with the Jet Propulsion Laboratory, California Institute of Technology, Pasadena, CA 91109 USA (telephone: 818-354-3272, e-mail: leif.scheck@jpl.nasa.gov).
F. Novak is with the Langley Research Center, NASA, Hampton, VA 23681-2199 USA (telephone: 757-864-1862, e-mail: f.j.novak@larc.nasa.gov).

Dark current is the signal that an optical device reports in the absence of light. Radiation increases dark current by either damaging the photonic collection site or damaging the oxide in the peripheral readout circuitry, which generates leakage. Active pixel sensors are very susceptible to these effects and dark current increase due to irradiation is the dominant problem in space applications of active pixel sensors [6]-[9]. Since some radiation species generate displacement damage more readily than others, the relative effect of radiation on an active pixel sensor is very complex. Protons, neutrons, and heavy ions will cause displacement damage as well as ionization damage. Very high energy electrons will also cause displacement damage. Displacement damage reduces the charge collection efficiency of the active pixel sensor [10],[11].

The circuit of the typical 3T photodiode APS cell is illustrated in Fig. 1. Light incident on the photodiode changes the current that passes through the photodiode and thus the voltage at the column output line is modulated. Radiation damage to the photodiode or any transistor in a 3T APS cell will cause leakage and increase dark current [2]. Due to manufacturing and other die level variances each cell has a unique dark current, and each cell will have a response independent of the rest of the array. Therefore, the device will respond to radiation damage across the device and to damage on a small volume, i.e. microdose. Gamma irradiation, as an example of a continuous dose field, will induce a rise in microdose across the device and each cell's response will be approximately proportional to the response of the whole. Heavy ion irradiation, on the other hand, will induce a rise in dark current in some of the APS cells of greater magnitude than the average increase of the device. These highly damaged cells are analogous to Single Hard Errors (SHE) in memories and are generally referred to as hot pixels. The false signal reported by the hot pixel presents several challenges to operation in a radiation environment.

APS devices have been studied for a wide variety of dark current issues [6]-[9]. The general effects of total dose irradiation have been the most scrutinized. General reliability issues that relate to dark current generation have also been investigated. Charge coupled devices have been studied for hot pixel effects [10],[11].

The level of integration in the modern 3T APS devices significantly increases the number of sensitive volumes on the device that are susceptible to ion strikes. The photodiode is liable to displacement damage. The RESET and gain transistors are susceptible to ionization damage. A damaged photodiode will source more current. Damaged transistors will tend to leak more and raise dark signal. Photosensitive devices are much more sensitive to displacement damage than CMOS support transistors. This raises the question of how heavy ion hits on the APS cell will damage and therefore affect the dark current reading in an APS cell.

Since ions will produce a highly localized damage pattern, the effects are described by microdosimetry as well as

dosimetry. Heavy ions produce displacement damage as well as localized ionization damage so the concept of non-ionizing energy loss (NIEL) is useful to employ. Heavy ions have the ability to induce both ionization damage and displacement damage. Ion strikes on ionization damage susceptible structures, like gate and field oxides, will induce damage and strikes on lightly doped collection volumes, which are sensitive to displacement damage, will also induce damage. Ionization damage is best described by LET and displacement damage is best described by NIEL.

The amount and profile of ionization depends on LET, atomic weight, energy of the ion, as well as device parameters and architecture. An ion will contribute to the displacement damage through the NIEL deposition. The magnitude of the shift in dark current, therefore, should be dependent on LET, or NIEL, of the ion. This study determines the dependence of anomalously large shifts in dark current, i.e. hot pixels, as a function of LET and predicts the damage mechanism due to heavy ions. The APS array is expected to exhibit behavior similar to IC arrays seen in other studies [12].

III. PROCEDURE AND SETUP

The devices used in this study were CC256PD APS fabricated from a JPL design. The imaging array consisted of a 512 by 512 array of 3T active pixel sensors. The CMOS devices were built on a 0.6 μm HP process. This device is a completely digital, so the signal from each APS cell is reported digitally on the output pins. This allows for temperature compensation of dark current. The peripheral circuitry sets integration time and data is clocked out synchronously with a clock input. For this study, a PC interrogated the device using a LABVIEW based code. The pixel size is 12 μm by 12 μm with a fill factor of 44%. The full well capacity is 2.4×10^{-14} C. The output range is 1.63V. The charge collection gain is the ratio of output voltage to charge collected and is 4.2 $\mu\text{V}/\text{e}$ at the photodiode. The ADC consists of a radiation hardened 10 bit 225 kHz device. The maximum data acquisition rate is 20 Mpixels/s. Therefore, the minimum integration time is equal to the frame read time or 300ms.

Fig. 2a shows a standard dark image of a virgin device. The vertical stripes in the image are due the variance in the offset of the access and readout circuitry. An image like the one shown in Fig. 2a is often taken as a baseline to reduce false signal. A continuous radiation field will increase the dark signal of all cells approximately equally. Different types of radiation will cause the standard deviation of radiation effects in cells to increase at different rates [13]-[14].

For this experiment, the biased devices were irradiated while operating. Dark current measurements were taken for several modes. The fixed pattern noise (FPN) and the dark current were the primary metrics. Two different integration times were also set to measure dependence on the integration time. The operating bias was set to 5 volts and the operating temperature was held at -25°C throughout the study.

Two identical dark current distributions histograms are plotted in Fig. 3. Both plots were measured from the same virgin chip at different times. The abscissa of Fig. 3 is the

dark rate at which each cell in the APS reports when read. The ordinate of Fig. 3 is the number of cells that report that dark rate. The distributions are quite similar. The similarity between them is more precisely shown by the distribution of differences in dark current each APS cell reported during the two reads, which is shown in Fig. 4. The distribution shown in Fig. 4 is narrow and symmetric, which indicates that anomalous rises in dark current will be easily seen. The non-zero mean of the distribution is typical of noise in ADC of this device. Also, any change in distribution parameters, e.g. variance of the fixed pattern noise, will also be measured for microdosimetry analysis.

For this study, three types of radiation were used. Gamma radiation was obtained at the JPL Co-60 source. Crocker Nuclear Laboratory supplied the protons used in this study. Brookhaven National Laboratory provided heavy ions. Gamma and proton radiation were employed to study the total ionizing dose effects on the devices. The TID study provided a calibration to which the effect of heavy ion irradiation could be compared. This comparison is pivotal since the gamma irradiation only induces ionization damage and an insignificant amount of displacement damage. Proton radiation, on the other hand, has a large displacement damage contribution. The ratio of ionization damage to displacement damage from proton irradiation can be changed in the device by operating the device in different bias modes. In this study, the proton irradiation occurred in biased and unbiased modes to modulate the amount of ionization damage. Unbiased oxides will accrue less damage than biased oxides while displacement damage occurs regardless of applied field. Irradiating devices in both the biased and unbiased modes allows for the differentiation between ionization and displacement damage.

Since NIEL may be a more apt metric for single particle dose depositions, NIEL is calculated using the method shown in [15] and by using TRIM. For these ions, the ratio between LET and NIEL is almost a constant. Galactic cosmic rays are known to have a divergent NIEL value for these events. Table I lists the NIEL and LET for the ions used.

TABLE I: SUMMARY OF TEST ION PARAMETERS.

Particle Type	Range in Si	LET in Si	NIEL in Si
	(μm)	($\text{MeV}\cdot\text{cm}^2/\text{mg}$)	($\text{MeV}\cdot\text{cm}^2/\text{g}$)
54 MeV Protons	1.40×10^4	9.30×10^{-3}	3.90×10^{-3}
56 MeV Li	365	0.375	0.12
99 MeV C	180	1.46	0.44
140 MeV F	116	3.54	1.1
125 MeV F	99	3.8	1.2
182 MeV Si	74	7.9	2.8
210 MeV Cl	64	11.5	4.3

253 MeV Ti	53.2	19.87	7.68
280 MeV Ni	42	28	14
305 MeV BR	83.7	37.47	22.5
385 MeV Au	30	81	125

The procedure of this test was to irradiate several devices. Four devices were irradiated with gamma radiation, three devices were irradiated with protons, and three devices were irradiated with heavy ions. One of the proton irradiations was unbiased. The FPN and dark current were measured between irradiation steps. The supply current and other CMOS parameter were monitored to ensure integrity of the read out circuitry. All irradiations occurred at normal incidence.

Dosimetry and micro-dosimetry studies for devices are fairly standardized [13],[14]. All of the devices are measured for macro-response, i.e., the supply current, average dark current and other average measurements are taken. This is the dosimetry measurement and it occurs for proton, gamma, and heavy ion radiation. A comparison will be made between the heavy ion, gamma, and proton result to discern whether the heavy ion induces damage like proton or gamma radiation. This result reveals the mechanism of hot pixels in the APS. For the micro response study, measurements similar to the macro study are performed on each cell. Parameters like the standard deviation can be extracted from these ensembles and used to predict device behavior. From these distributions extremely rare events, i.e., cells demonstrating extreme radiation damage, can be identified and measured. APS and CCD cells that exhibit a dark signal that is six standard deviations above the mean of the distribution has been typically considered a “hot pixel.” For example, in Fig. 4, the standard deviation is 4 V/s, so any shifts in dark current over 24 V/s from the mean would be considered a hot pixel. Hot pixel response is then measured as a function of fluence, LET, or NIEL. From these measurements, the response of the device as a dosimeter and microdosimeter can be ascertained.

All radiation types will tend to increase the average dark current of the cells. Therefore, a highly dosed cell may look less and less like a hot pixel as the device is irradiated. So for this study, small dose levels were used and readouts were taken at each level. In this manner, the generation of hot pixels is easily analyzed for low dose amounts. This is mathematically equivalent to the cross section being the slope of hot pixels as a function of fluence, or

$$\sigma \equiv \frac{dN}{d\Phi}, \quad (1)$$

where N is the number of hot pixel that are greater than six standard deviation above the mean and Φ is the fluence. Since a dosed part may result in overall average shift distributions that are within six standard deviations of the saturation level, these events fail the definition of hot pixels. Ion run results that exhibit this behavior are not used to

calculate microdose behavior. Therefore, total dose from ions is kept low in these studies. This is the typical approach for microdose damage studies [13].

IV. RESULTS

The first section of data analyzes the dark current TID response of the devices. Fig. 5 plots the average dark rate of a DUT for gamma, proton, and heavy ion irradiations. Identical test protocols were followed for all DUTs. It is obvious from comparing the curves in Fig. 5 that the displacement damage induced by protons affects the dark current much differently than the gamma radiation that is ionization damage only. The proton induced dark current saturated relatively quickly. The damage from gamma continues to accrue until the DUT failed. All devices were seen to fail from total dose around 100 krad(Si). Heavy ion total dosing was seen to increase dark rate in a similar fashion to protons radiation, implying that the damage due to heavy ions is the same type of damage caused by proton radiation, i.e., displacement damage.

Fig. 6 plots the distributions of dark rate for various dose levels of protons. The distribution gets wider and the mean shifts higher with dose. This is typical of microdosimetric response in cell arrays [7]. Fig. 7 shows the mean and standard deviation of the curves in Fig. 6 as a function of dose. The distribution mode and average value are shifted higher, which is a total dose effect. Also, the distribution variance has increased, i.e., the distribution is wider, and there are many outliers, which is a microdosimetry effect.

Fig. 8 shows the shift spectra, which is generated in the same way as Fig. 5, before and after an irradiation. The number of hot pixels is determined by counting the number of shifts in Fig. 9 with value greater than six standard deviations over the mean of the distribution. Figs. 9 and 10 plot the number of hot pixels as a function of fluence for 60 MeV protons and 300 MeV Bromine ions, respectively. Both trends appear linear, which means the cross section of hot pixels is constant with respect to fluence. Other ion species induce similar behavior.

The slopes of Figs. 9 and 10 are equivalent to the cross section of a hot pixel. The cross section of different LET and energy particles can be found in this fashion. The results are plotted in Fig. 11 as a function of LET. This is the characteristic cross section curve for a hot pixel. The result of Fig. 11 allows the rate of hot pixels to be calculated. Fig. 12 shows the response of hot pixels to NIEL. The physical cross section of the photodiode is $3.7 \times 10^{-1} \text{ cm}^{-2}$. Since the cross section for hot pixels is much less than the physical cross-section, the mechanism for a hot pixel is obviously more complex than single hits on the photodiode.

V. CONCLUSIONS

A microdosimetry analysis of various ion irradiations of APS cells show that the response is not completely typical with a microdosimetric response. The number of hot pixels does not with LET or NIEL of the particle. The cross section of hot pixels is seen to be much smaller than the physical cross section. A rate calculation of hot pixels can only be calculated if the spectrum of space ions is known as a

function of NIEL, rather than LET. This relation was not currently known.

REFERENCES

[1] Chen, W., De Geronimo, G., Li, Z., O'Connor, P., Radeka, V., Rehak, P., Smith, G.C., Yu, B., "Active pixel sensors on high-resistivity silicon and their readout", Nuclear Science, IEEE Transactions on , Volume: 49 Issue: 3 , Jun 2002 Page(s): 1006 -1011

[2]. Purll, Adolph, Uwaerts, Weible, "A new technology attitude sensor", pp. 267-272, Feb. 2000 .

[3]. Liebe, Dennison, Hancock, Stirbl, Pain, "Active pixel sensor (APS) based star tracker", pp. 119-127, 1998.

[4]. Meynants, Dierickx, Scheffer, "CMOS active pixel image sensor with CCD performance", Proc SPIE, vol.3410, pp.68- 76, 1998.

[5]. Saint-Pe, Davencens, Tulet, Magnan, Cavadore, Gautrand, Degerli, Lavernhe, Farre, "Development and characterization of active pixel sensors for space applications", Proc SPIE, vol.3440, pp.24-36, 1998.

[6] Bogaerts, J., Dierickx, B., Mertens, R., "Enhanced dark current generation in proton-irradiated CMOS active pixel Sensors", Nuclear Science, IEEE Transactions on , Volume: 49 Issue: 3 , Jun 2002, Page(s): 1513 -1521

[7] Hopkinson, G.R., Dale, C.J., Marshall, P.W., Proton effects in charge-coupled devices Nuclear Science, IEEE Transactions on , Volume: 43 Issue: 2 , Apr 1996 Page(s): 614 -627.

[8]. Hancock, Soli, "Total dose testing of a CMOS charged particle spectrometer", vol.44, pp. 1957-1964, Dec. 1997.

[9]. Cohen, David, "Radiation effects on active pixel sensors", pp.450- 456, 2000.

[10]. Hopkinson, "Radiation-induced dark current increases in CCDs", pp.401-408, 1994.

[11]. Hopkinson, "Proton irradiation induced RTS in CCDs", Proc 14th Int. Conf. On Noise in Physical Systems and 1/f Fluctuations , World Scientific, Singapore, pp.218-223, 1997.

[12] Belredon, X., David, J., Lewis, D., Beauchene, T., Pouget, V., Barde, S., Magnan, P., "Heavy ion-induced charge collection mechanisms in CMOS active pixel sensor," Nuclear Science, IEEE Transactions on , Volume: 49 Issue: 6 , Dec 2002 Page(s): 2836 -2843

[13] Scheick, L.Z., Swift, G.M., Dose and microdose measurement based on threshold shifts in MOSFET arrays in commercial SRAMs Nuclear Science, IEEE Transactions on , Volume: 49 Issue: 6 , Dec 2002 Page(s): 2810 -2817

[14] Xapsos, M. A."Hard Error Distributions of Gate Oxide Arrays in the Laboratory and Space Environments," Nuclear Science, IEEE Transactions on , Volume: 43 Issue: 2 , Apr 1996 Page(s): 3139.

[15] S.R. Messenger, E.A. Burke, G.P. Summers, M.A. Xapsos, R.J. Walters, E.M. Jackson, and B.D. Weaver, "Nonionizing Energy Loss (NIEL) for Heavy Ions," *IEEE Trans. Nucl. Sci.*, vol. 46, pp. 1595-1602, Dec. 1999.

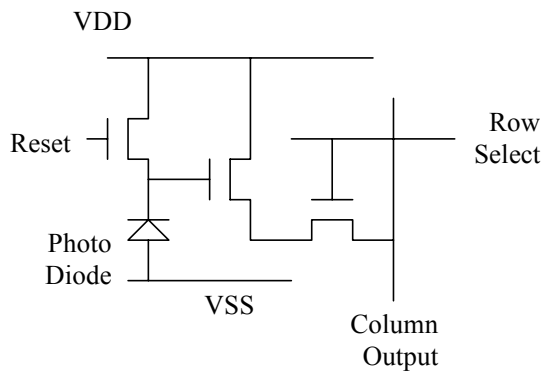


Fig. 1. A photodiode based 3T active pixel sensor.

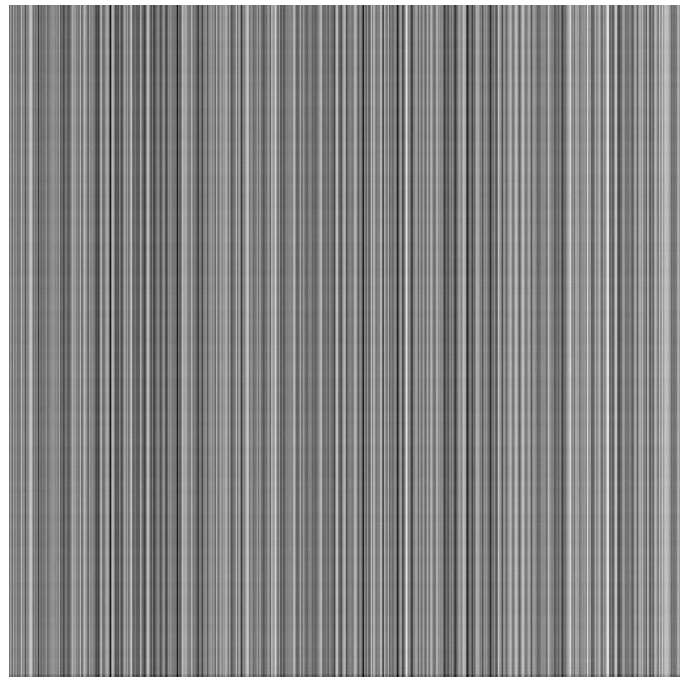


Fig. 2a An APS image of virgin device.

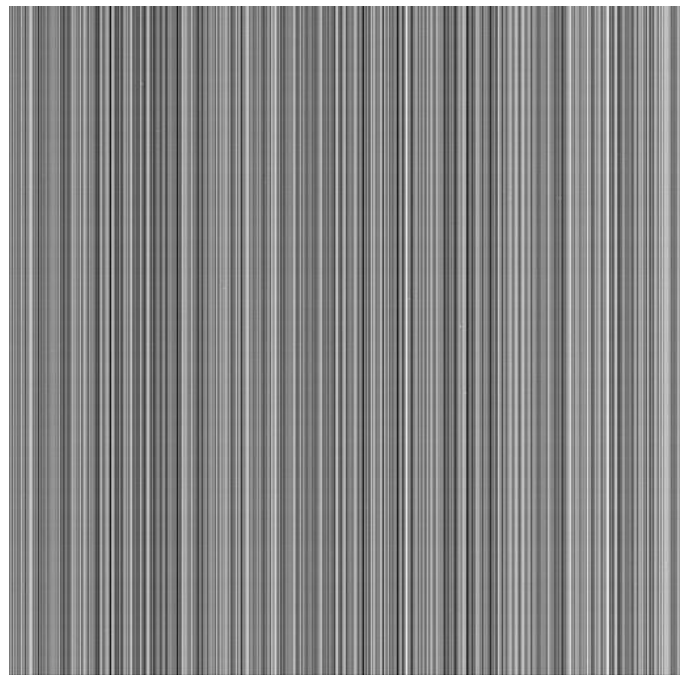


Fig. 2b An APS image of a device irradiated with 1×10^4 ions cm^{-2} .

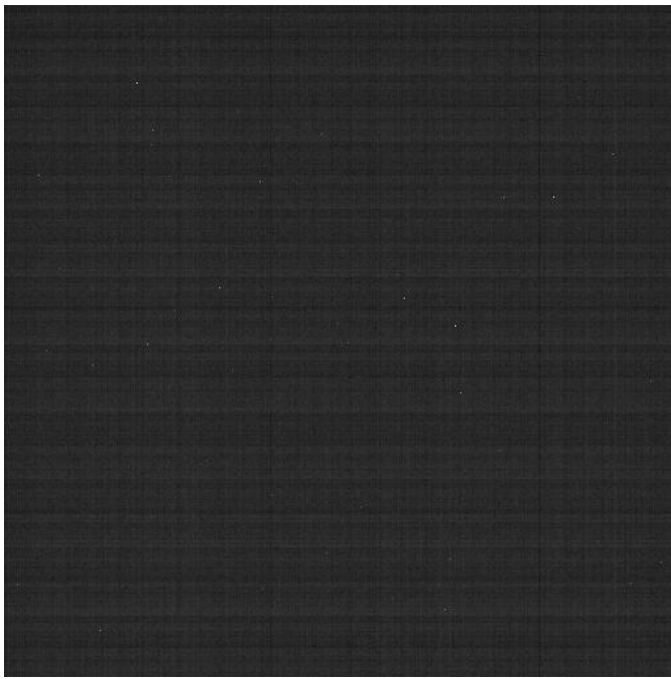


Fig. 2c Result of virgin device image removed from irradiated image. Individually irradiated pixels are the white dots.

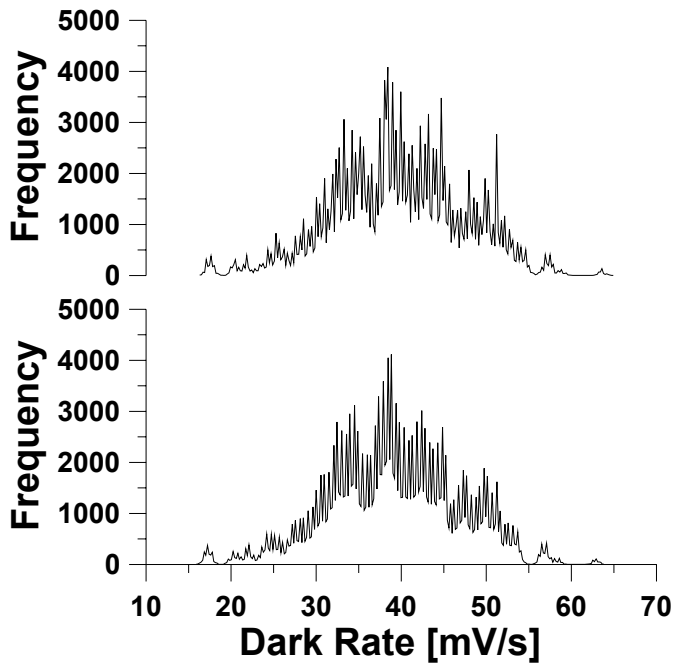


Fig. 3. Distribution of dark signal across the APS for two reads of virgin devices.

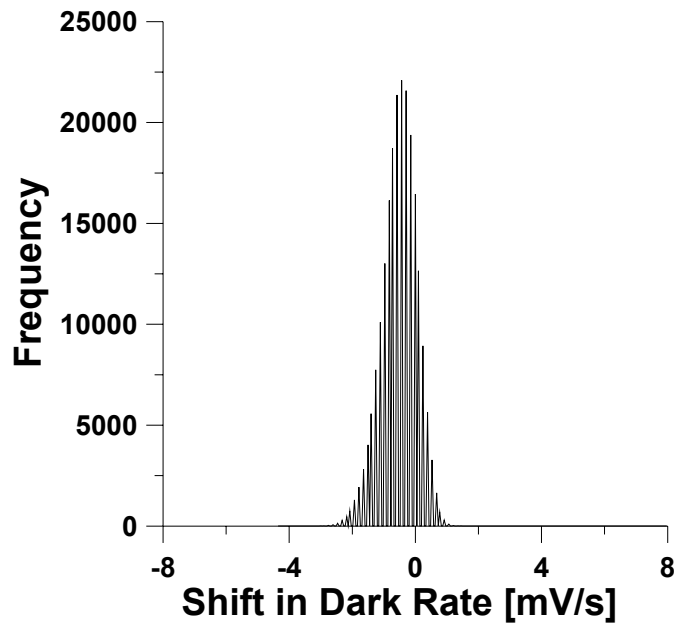


Fig. 4. Distribution of variance across an APS device, which is also the noise on a single cell.

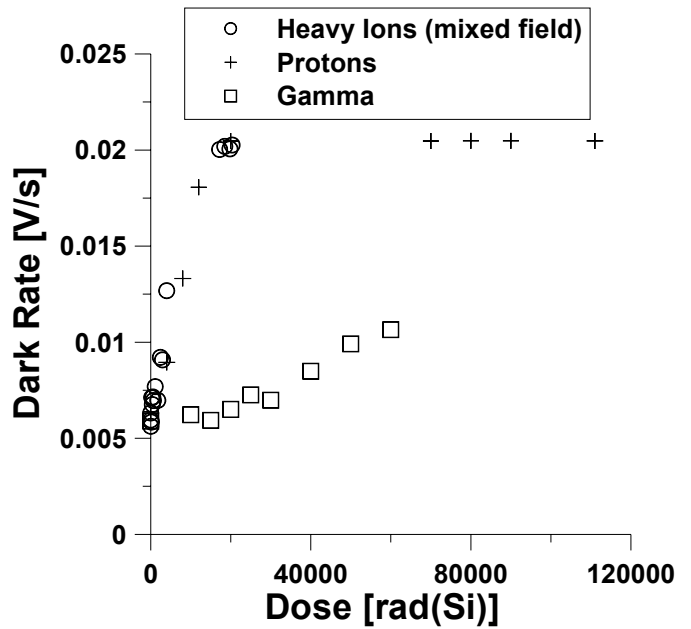


Fig. 5. Dark signal response to total dose.

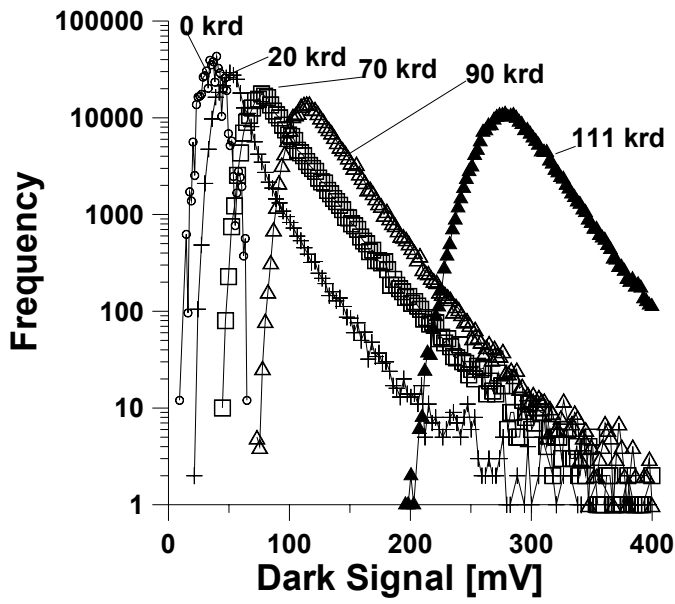


Fig. 6. FPN distribution due to proton irradiation.

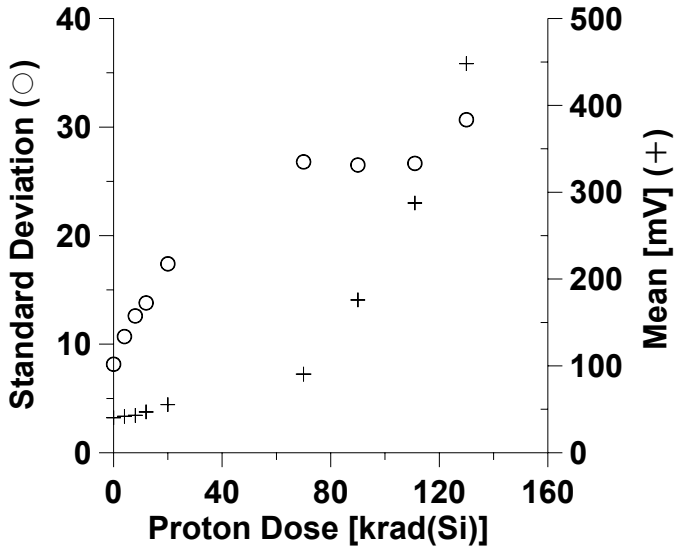


Fig. 7. Mean and standard deviation of FPN distributions as a function of proton dose.

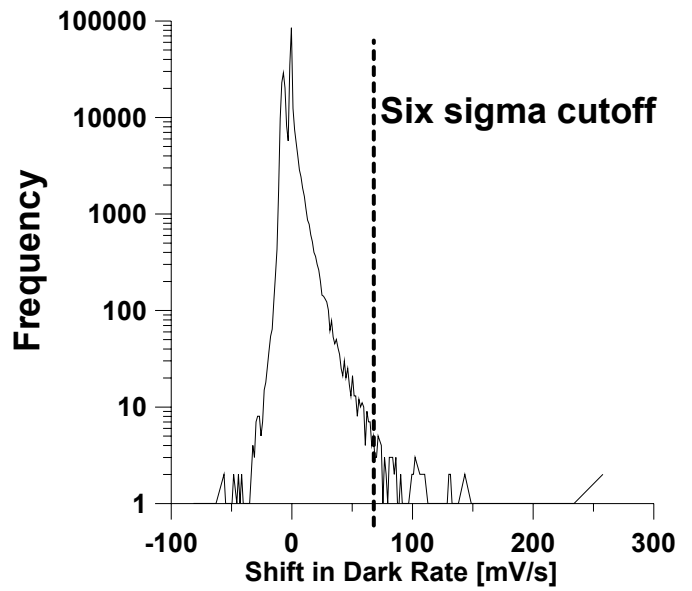


Fig. 8. Shift in dark current response across the APS due to $8 \times 10^5 \text{ cm}^{-2}$ gold ions.

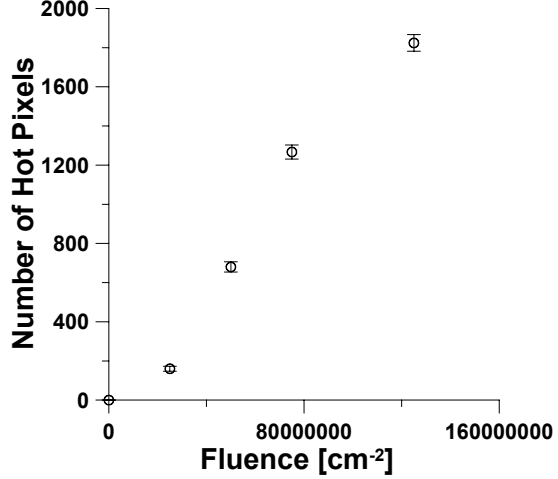


Fig. 9 Development of hot pixel as a function of dose for protons. The slope here is $1.5 \times 10^{-5} \text{ cm}^{-2}$ which is also the proton cross section of a hot pixel for this energy proton.

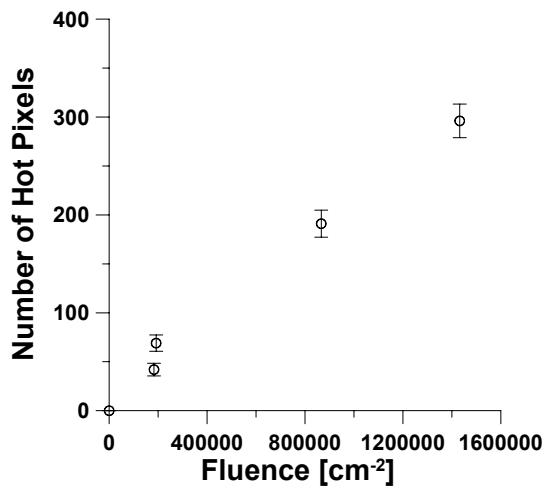


Fig. 10. Development of hot pixel as a function of dose for heavy ions. The slope here is $3.14 \times 10^{-4} \text{ cm}^2$ which is also the ion cross section of a hot pixel for this NIEL ion.

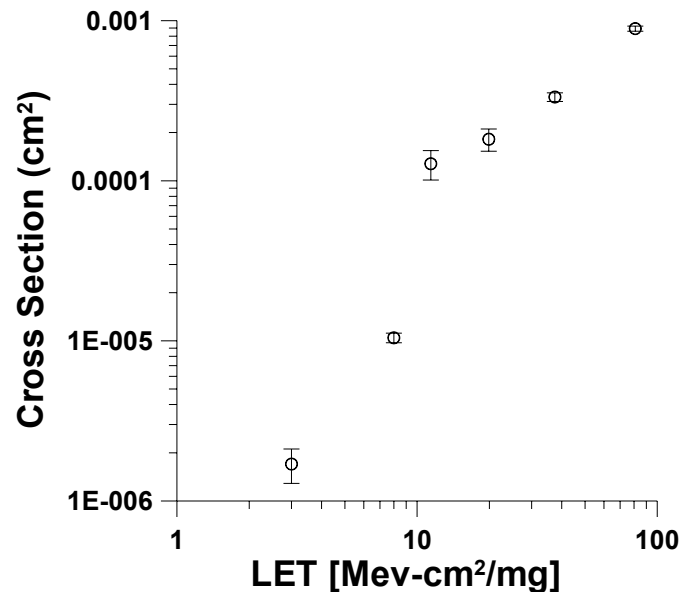


Fig. 11. Cross section of hot pixels as a function of LET.

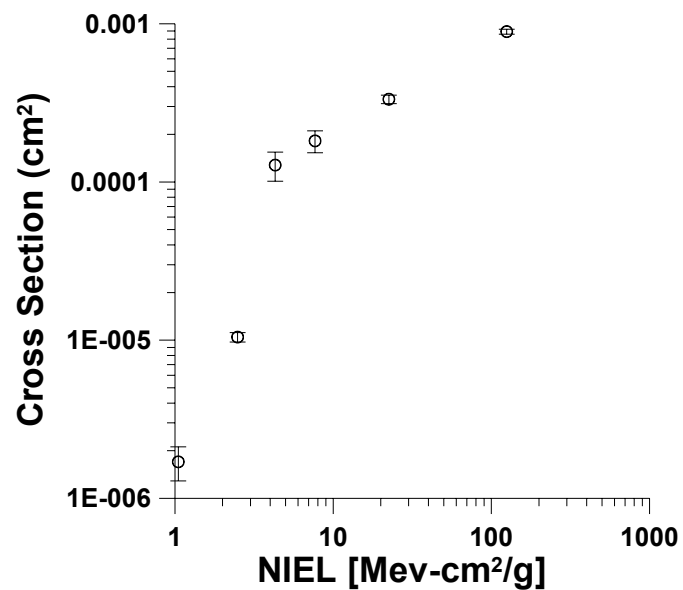


Fig. 12. Cross section of hot pixels as a function of NIEL.